

Sensor and Simulation Notes

Note 287
18 July 1985

FIELD - CONTAINING INDUCTORS

Y.G. Chen, R. Crumley
Maxwell Laboratories, San Diego, CA

Carl E. Baum
Air Force Weapons Laboratory

and

D.V. Giri
Pro-Tech, 125 University Avenue, Berkeley, CA 94710

Abstract

Field - containing inductors are required in certain simulator applications e.g., elements of pulse shaping networks, terminators for transmission lines etc. Typical coils such as solenoids have a large magnetic dipole moment resulting in excessive interfering magnetic fields. An improved design based on the traditional toroidal coil windings is presented. This new design consisting of two windings is capable of higher voltage operation. Optimal shapes, energy and forces exerted are also discussed. The normalized plots of attainable inductance for varying geometrical parameters presented in this note should prove useful in future designs and applications.

Sensor and Simulation Notes

Note 287

18 July 1985

FIELD - CONTAINING INDUCTORS

Y.G. Chen, R. Crumley
Maxwell Laboratories, San Diego, CA

Carl E. Baum
Air Force Weapons Laboratory

and

D.V. Giri
Pro-Tech, 125 University Avenue, Berkeley, CA 94710

Abstract

Field - containing inductors are required in certain simulator applications e.g., elements of pulse shaping networks, terminators for transmission lines etc. Typical coils such as solenoids have a large magnetic dipole moment resulting in excessive interfering magnetic fields. An improved design based on the traditional toroidal coil windings is presented. This new design consisting of two windings is capable of higher voltage operation. Optimal shapes, energy and forces exerted are also discussed. The normalized plots of attainable inductance for varying geometrical parameters presented in this note should prove useful in future designs and applications.

Keywords: transmission lines, solenoids, magnetic fields



CONTENTS

<u>Section</u>		<u>Page</u>
I.	INTRODUCTION	3
II.	GENERAL CONSIDERATIONS	7
III.	SOLUTION FOR BODIES OF REVOLUTION	11
IV.	TOROIDS WITH RECTANGULAR CROSS SECTION	15
V.	OPTIMUM SHAPE FOR CONTAINMENT IN FINITE SPHERICAL VOLUME AND OTHER PERFORMANCE CHARACTERISTICS	22
VI.	SUMMARY	29
	REFERENCES	30

I. INTRODUCTION

Field - containing inductors are useful in certain simulator applications, e.g., pulse-shaping networks and lumped-element terminations for transmission lines. If the magnetic field produced by the current flow in the inductor is not contained, the exterior magnetic field from such an inductor could adversely impact the simulated environment. A second example is when there are different pulse generators (drivers) designed to produce the required environment in different time regimes (early time and late time drivers), one has to be cautious of the compatibility between the sources. If lumped elements such as inductors are used in one driver or in connecting the two (or more) drivers, it should not adversely impact the performance of the other driver(s) via magnetic coupling.

In view of the above outlined need, it is the purpose of this note to formulate the design principles for a field containing inductor, for high voltage applications. In this introductory section, the classical solenoidal inductor is reviewed to indicate the presence of external magnetic field, which could be excessive.

Consider a long solenoid of length l and winding radius a as shown in its cross section in figure 1.1. Both rectangular (x, y, z) and cylindrical (ψ, ϕ, z) coordinates are useful for this geometry as indicated in figure 1.2. In addition, the general appearance of its magnetic field is shown in figure 1.3. It is relatively easy to determine its inductance especially under the assumption of negligible end effects. The inductance L_s is defined as the magnetic flux linkages Λ divided by the current I causing the flux. The number of flux linkages is of course given by the sum over all the N turns of the magnetic fluxes ϕ_n in each turn, or

$$L_s = \frac{\Lambda}{I} = \frac{1}{I} \sum_{n=1}^N \phi_n \cong \frac{N\phi}{I} \quad (1.1)$$

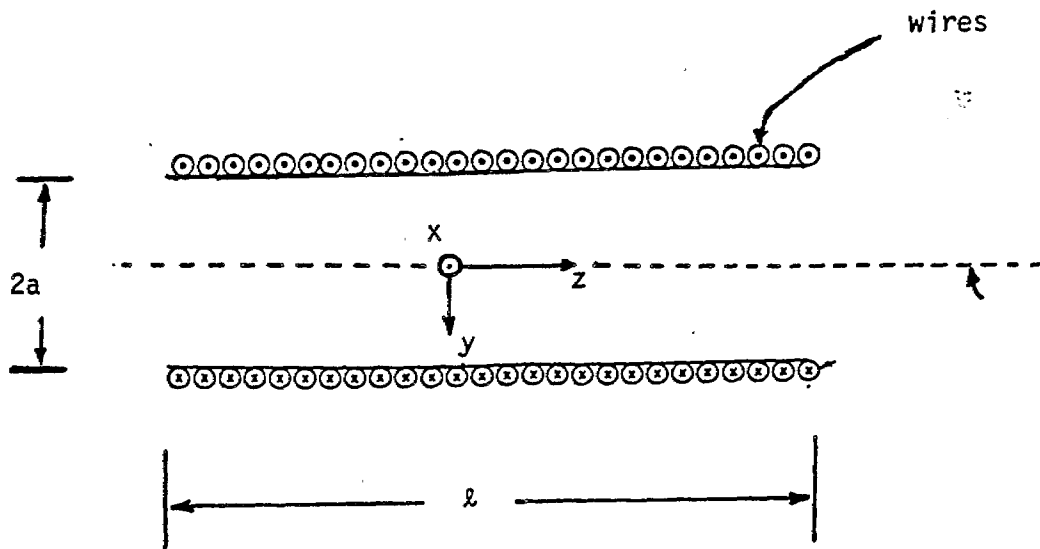


Figure 1.1 Cross sectional view of a long solenoidal winding.

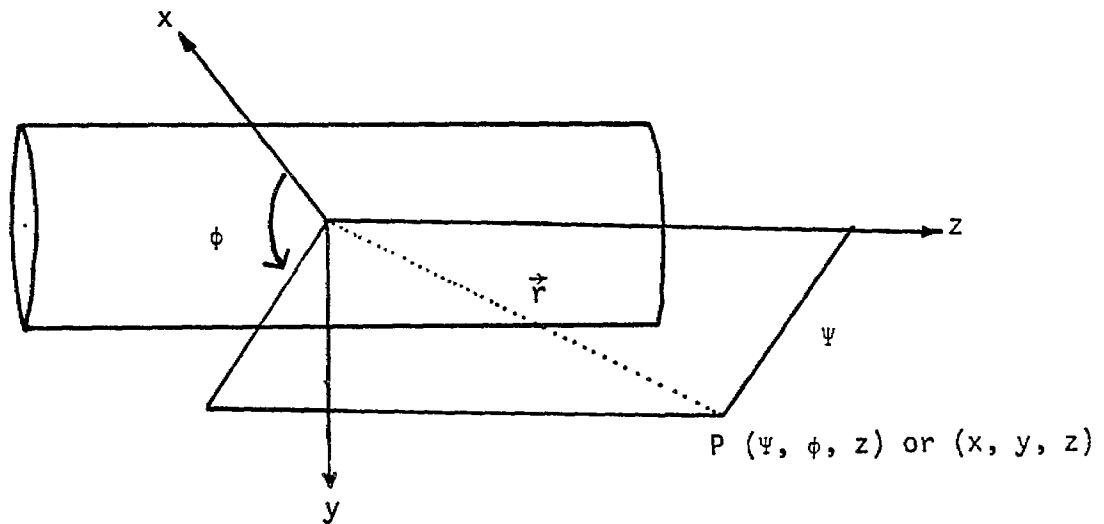


Figure 1.2 Rectangular and cylindrical coordinate system.

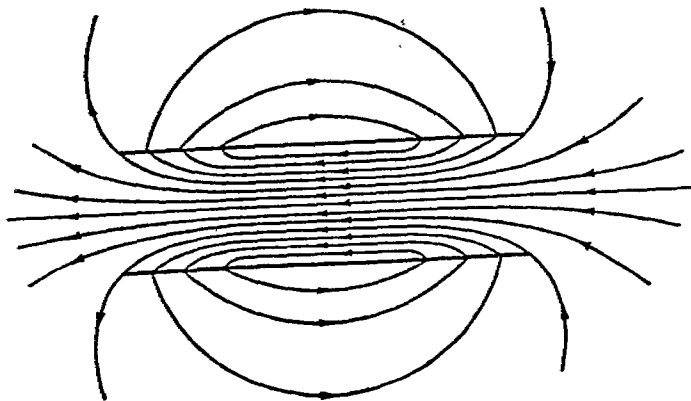


Figure 1.3 General appearance of the magnetic field.

The magnetic induction B inside the long solenoid is fairly constant and is given by

$$B \cong \mu_0 N' I \quad (1.2)$$

where $N' =$ number of turns per unit length. Therefore

$$\Phi \cong \mu_0 \frac{N}{\ell} I \pi a^2 \quad (1.3)$$

leading to

$$L_S \cong \frac{N\Phi}{I} \cong \mu_0 \frac{N^2}{\ell} \pi a^2 = \mu_0 N'^2 \ell \pi a^2 \quad (1.4)$$

Having reviewed the inductance L_S of the solenoid, we may estimate the magnetic field at a distant observation point. At low frequencies, the quasi-static magnetic field \vec{H}_S from the solenoid current is dominated by the magnetic dipole moment \vec{m} , which is given by

$$\begin{aligned} \vec{m} &= \vec{i}_z m_z \\ &= \vec{i}_z N I \pi a^2 \end{aligned} \quad (1.5)$$

The quasi-static magnetic field from such a dipole moment at a general position vector \vec{r} is given by [1],

$$\vec{H}_S(\vec{r}) \cong \frac{1}{4\pi r^3} [3\vec{i}_r \vec{i}_r - \vec{1}] \cdot \vec{m} \quad (1.6)$$

where

$$\vec{i}_z = \text{unit vector in } z \text{ direction} \quad (1.7)$$

$$\vec{1} \equiv \vec{i}_x \vec{i}_x + \vec{i}_y \vec{i}_y + \vec{i}_z \vec{i}_z \equiv \text{identity dyadic}$$

The magnitude of the distant quasi-static magnetic field is then bounded by

$$\left| \vec{H}_s(r) \right| \leq \frac{N a^2 I}{2r^3} \quad (1.8)$$

In addition to the above solenoidal field, one also has an azimuthal magnetic field $\vec{H}_{\ell\phi}$ due to the current I flowing in the lead wires, which is simply given by

$$\vec{H}_{\ell\phi} = \vec{I}_{\phi} H_{\ell\phi} \quad \text{and} \quad H_{\ell\phi} = I/(2\pi \psi) \quad (1.9)$$

Considering a ratio of field due to the solenoid and the field due to the lead wire, we have

$$\frac{\left| \vec{H}_s(r) \right|}{H_{\ell\phi}} \leq \frac{N\pi\psi a^2}{r^3} \quad (1.10)$$

Because of the factor N , which is typically large, it is observed that the field due to the solenoid could far exceed the field due to the current in the lead wires entering and exiting the solenoid. Such excessive magnetic field could interfere with other parts of circuits in which such solenoidal inductors are employed. Such interference may not be tolerable in certain simulator applications, thus leading to a requirement of field - containing inductors, that can also possess high-operating-voltage capabilities, which is the subject of this note.

In concluding this section, we remark on how the note is organized. Certain general topological considerations on field containment are discussed in Section II and a solution for a general body of revolution is presented in Section III. Toroidal forms with rectangular cross section is the subject of Section IV. Given such a toroidal form, certain optimization procedures, considerations of energy and forces exerted due to the current flow are discussed in Section V. The note is concluded with a summary in Section VI followed by a list of references.

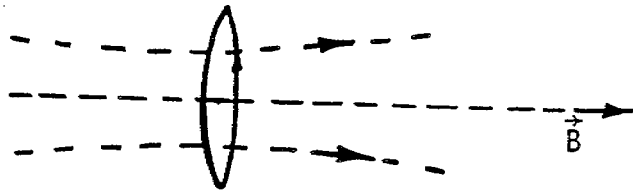
II. GENERAL CONSIDERATIONS

Since the object is to provide design guidelines for a magnetic - field - containing inductor, it is desirable to review the general behavior of magnetic fields. Since isolated magnetic charges are not yet found, the divergence of the magnetic field is taken to be zero, i.e.,

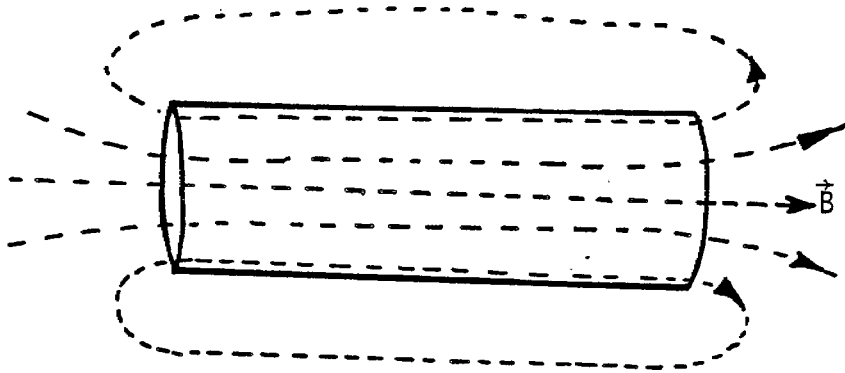
$$\nabla \cdot \vec{B}(\vec{r}) = \mu \nabla \cdot \vec{H}(\vec{r}) = 0 \quad (2.1)$$

where \vec{B} and \vec{H} stand for magnetic flux density and field intensity respectively and the permeability μ of the medium is assumed to be uniform. Physically, the above equation requires that the magnetic field lines are closed loops, since there are no isolated magnetic charges upon which they can terminate. To illustrate the vanishing divergence of the magnetic field and also the general appearance of magnetic fields, let us consider several shapes of perfectly conducting surfaces as illustrated in figure 2.1. Note that at a perfectly conducting surface the normal component of the magnetic field is zero. For example, figure 2.1a shows a single turn of current and its associated magnetic field. Several such turns arranged together leads to the tubular 'conductor' of figure 2.1b. The magnetic field lines now are closed and parallel to the conductor, satisfying the boundary condition on the normal component. Figure 2.1c is an example of a bent tubular conductor leading finally to a closed surface of figure 2.1d, that could contain the field. Assuming a perfectly conducting surface, the surface current on this closed surface is whatever is needed to satisfy the boundary conditions. Such a closed surface could have a \vec{B} outside, but it is not essential to have an external field, since a zero external magnetic field automatically satisfies the boundary condition on its normal component, i.e. $B_n = 0$.

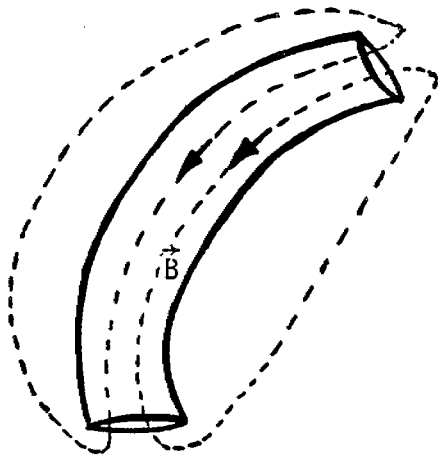
Having established that a closed surface, S , enclosing a volume V is required for field containment, one needs to consider the particular types



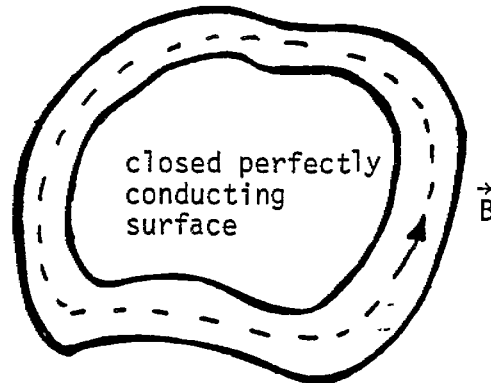
(a) Single turn of current with its magnetic field.



(b) Magnetic field associated with a tubular perfect conductor.



(c) Another example of tubular conductor.



No outside field is needed.

(d) Closed volume formed by a perfectly conducting surface.

Figure 2.1 General behavior of magnetic fields around perfectly conducting surfaces.

of closed surfaces suitable for field containment. Some examples are shown in figure 2.2 using the multiplicity number p , that characterizes any simple closed surface S [2].

It is easy to show that a simple closed surface $p = 0$ of figure 2.2a does not meet the requirement. Recall that a quasi-static magnetic flux density \vec{B} is a negative gradient of a scalar potential ϕ_m [3] i.e.,

$$\vec{B} = -\nabla\phi_m \quad (2.2)$$

which implies that

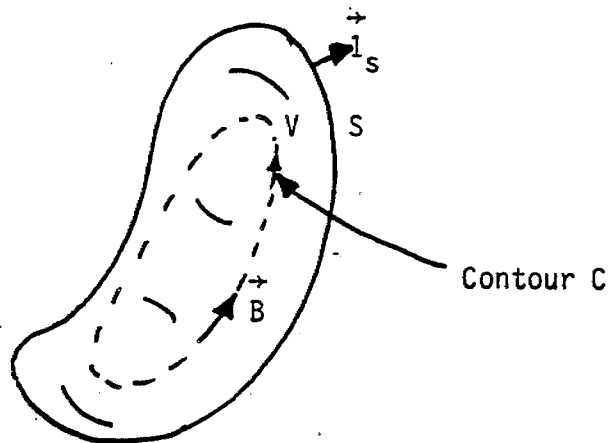
$$\begin{aligned} \nabla \times \vec{B} &= 0 \\ \nabla \times \vec{H} &= 0 \end{aligned} \quad (2.3)$$

and ϕ_m is the solution of the Laplace equation and not Poisson's equation owing to the absence of isolated magnetic charges. Also, from Maxwell's equations, we have

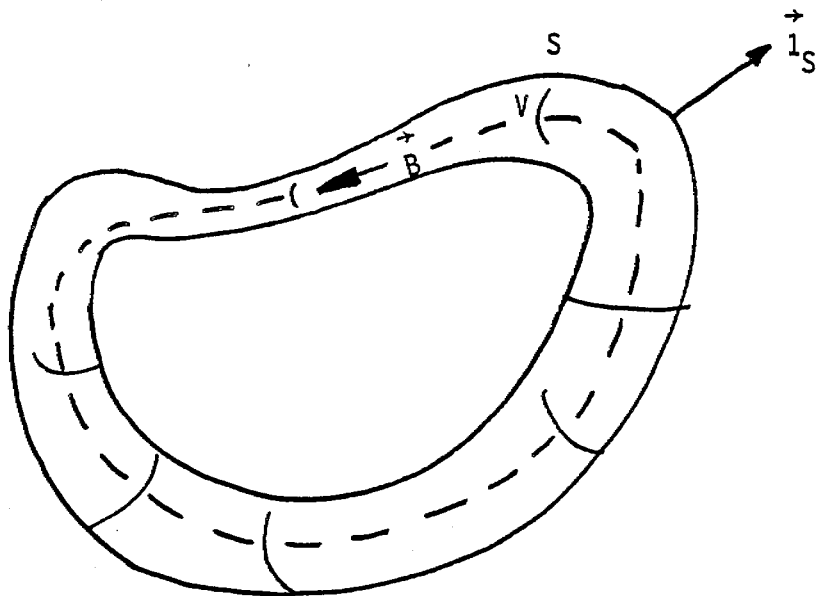
$$\nabla \times \vec{H} = \vec{J} + \frac{\partial \vec{D}}{\partial t}, \quad \oint_C \vec{H} \cdot d\vec{\ell} = \int_{S'} \left(\vec{J} + \frac{\partial \vec{D}}{\partial t} \right) \cdot d\vec{S}' = I_t \quad (2.4)$$

where the contour C is any closed line of \vec{B} , S' is a surface with boundary C , and I_t is the total current through S' . In the quasi-static limit $\partial \vec{D} / \partial t$ is negligible, so that $I_t = I$ (the current through S'). But the configuration of figure 2.2a has a non-zero value for I and therefore \vec{J} , contradicting (2.3). This requires that there be a current flow through S' . Since this is not possible in the absence of a conductor, one must have a closed current path, not in V , through which the magnetic field, and hence V , passes. Thus one is led to conclude that we need a surface that is multiply connected, i.e., $p \geq 1$. Putting it differently, the 'coil' we are designing could be thought of topologically as a sphere with 1 or more handles.

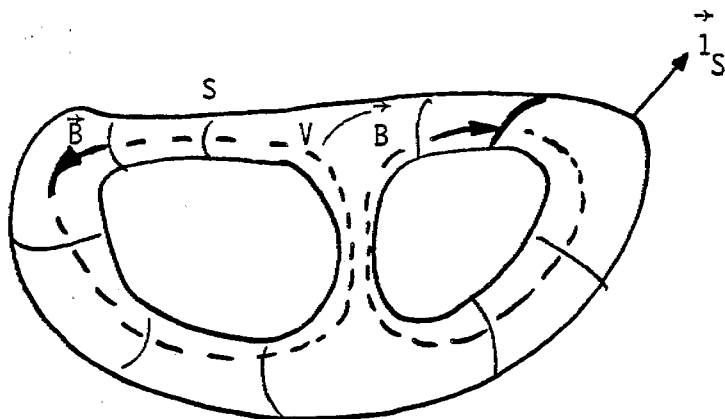
It is observed that a singly connected closed surface ($p = 1$) is the simplest of all permissible closed surfaces to meet the requirement on field containment. A solution to a general $p = 1$ surface or a body of revolution is the subject of the following section.



(a) Simply connected closed surface $p = 0$.



(b) Singly connected closed surface $p = 1$.



(c) Doubly connected closed surface $p = 2$.

Figure 2.2 Examples of multiply connected closed surfaces.

III. SOLUTION FOR BODIES OF REVOLUTION

In the previous section, we observed that a singly connected closed surface ($p = 1$) will meet our requirement of field containment while satisfying the boundary condition on the normal component of the magnetic field at a perfectly conducting surface. It is further observed that it is desirable to have a uniform cross section for this surface so that the current density is uniform also. The two criteria above along with a consideration of symmetry leads us to a generalized toroidal body of revolution as shown in figure 3.1.

Referring to figure 3.1, the magnetic field from such a current distribution is oriented in the azimuthal or ϕ direction and is inversely proportional to the cylindrical radius ψ as one moves away from the surface, according as

$$\vec{H} = \vec{1}_{\phi} \cdot H_{\phi} \tag{3.1}$$
$$H_{\phi} = \text{constant}/\psi$$

The above magnetic field comes from a solution of the Laplace equation and also satisfies the boundary condition. Of course $\psi > 0$ in the above, for $p = 1$, which is the case. The surface current density is then given by

$$\vec{J}_S = \vec{1}_S \times \vec{H} = \vec{1}_{\phi} H_{\phi} \tag{3.2}$$

or

$$J_{S\phi} = \text{constant}/\psi \tag{3.3}$$

The above general solution of a toroidal surface can now be applied to a coil requiring that the current density in the toroid be also inversely proportional to the radial distance. Figure 3.2 shows a section

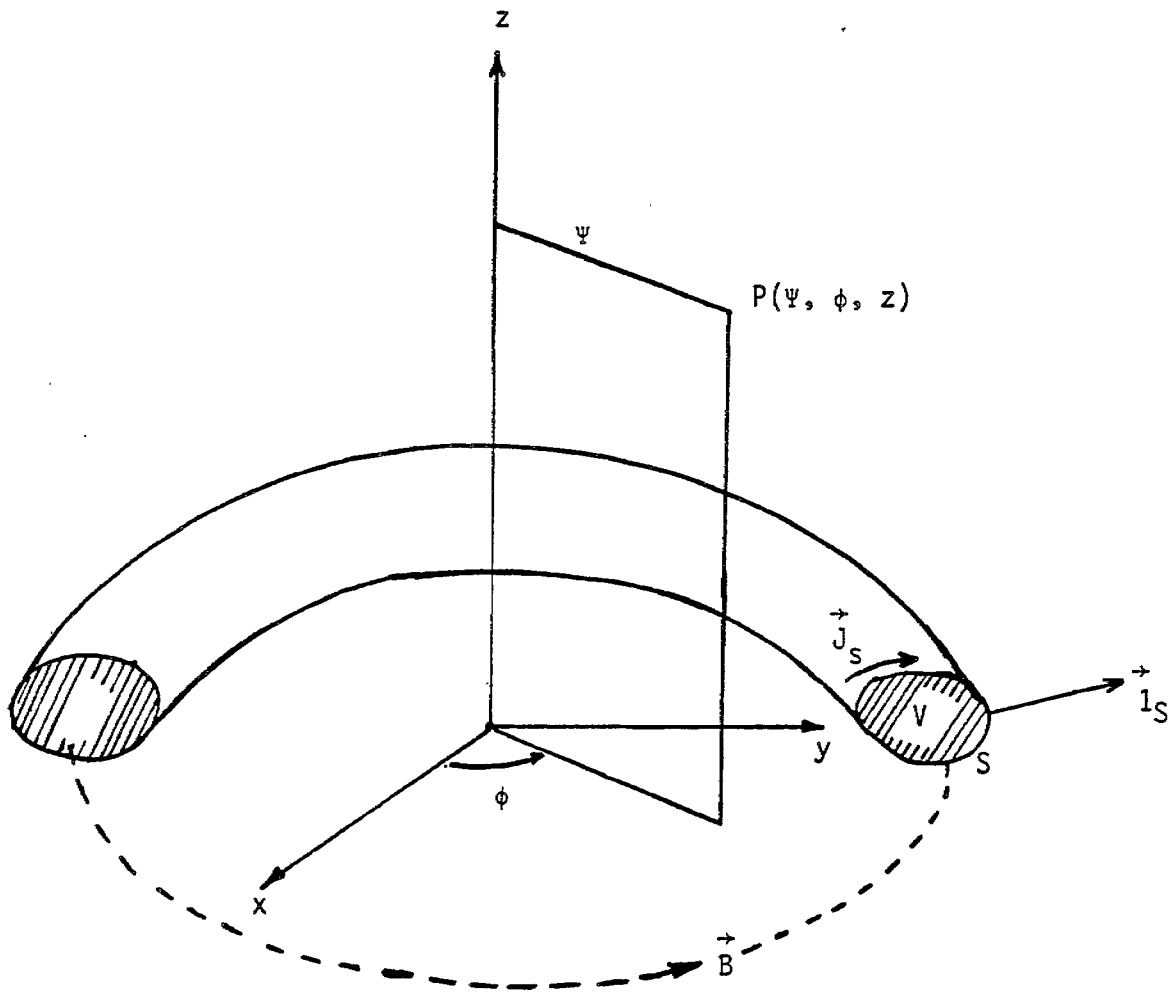
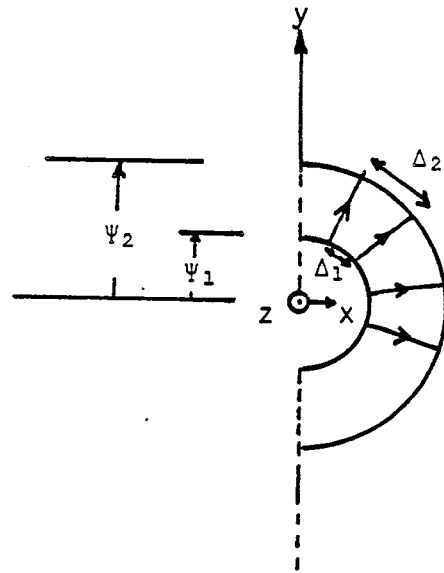


Figure 3.1 A generalized toroidal body of revolution and associated magnetic field.



inner spacing < outer spacing
 $(\Delta_1 < \Delta_2)$

Figure 3.2 Winding on a toroidal form showing the difference in current densities at inner and outer extremities.

of a toroidal form on which the wire carrying current I is wound. It is observed that the current densities at inner and outer extremities are approximately

$$\begin{aligned} J_{s1} &\cong I/\Delta_1 \quad , \quad J_{s2} \cong I/\Delta_2 \\ \Delta_1 &\equiv \text{inner spacing between turn centers} \\ \Delta_2 &\equiv \text{outer spacing between turn centers} \end{aligned} \tag{3.4}$$

If we maintain

$$\Delta_1 / \Delta_2 = \psi_1 / \psi_2 \tag{3.5}$$

then, we have the condition that the current densities which the turns approximate are inversely proportional to the cylindrical radius ψ . In other words, the insulating space between the adjacent turns (plus the turn thickness) at the inner and outer boundary should be in the same ratio as the inner and outer radii. This condition is easily met in actual fabrication.

In concluding this section, it is noted that the results of a perfectly conducting surface have been applied to a practical coil and the nature of adjusting the winding spacing is also determined. Based upon this toroidal form, the results for a specific toroid with a rectangular cross section are presented in the following section, for two different winding arrangements.

IV. TOROIDS WITH RECTANGULAR CROSS SECTION

Toroidal forms have been frequently used in fabricating inductors to obtain desired values of inductance. Typically, such inductors are wound on a ring shaped form (see figure 4.1) in a single layer as shown in figure 4.2. Such inductors have the advantage of very little external magnetic field. Formulas for the ideal case of a current sheet, such as would be attained by a winding of very thin tape with negligible insulating space between the turns are simple [4].

For the geometry of figure 4.2, using the Ampere's Law, we have

$$\oint_C \vec{B} \cdot d\vec{\ell} = \mu I(\text{enclosed}) \quad (4.1)$$

The current enclosed is simply the number of turns N_1 times the current through the wire, leading to the magnetic flux density in the toroidal form given by

$$B(\psi) = \frac{\mu N_1 I}{2\pi\psi} \quad (4.2)$$

The total magnetic flux in a cross section is then

$$\begin{aligned} \phi &= \int_{\psi_1}^{\psi_2} \int_0^w dz \frac{\mu_0 N_1 I}{2\pi\psi} d\psi \\ &= \frac{\mu}{2\pi} w N_1 I \ln \left(\frac{\psi_2}{\psi_1} \right) \end{aligned} \quad (4.3)$$

and the inductance L_1 is therefore given by

$$L_1 = \frac{N_1 \phi}{I} = \frac{\mu}{2\pi} w N_1^2 \ln \left(\frac{\psi_2}{\psi_1} \right) \quad (4.4)$$

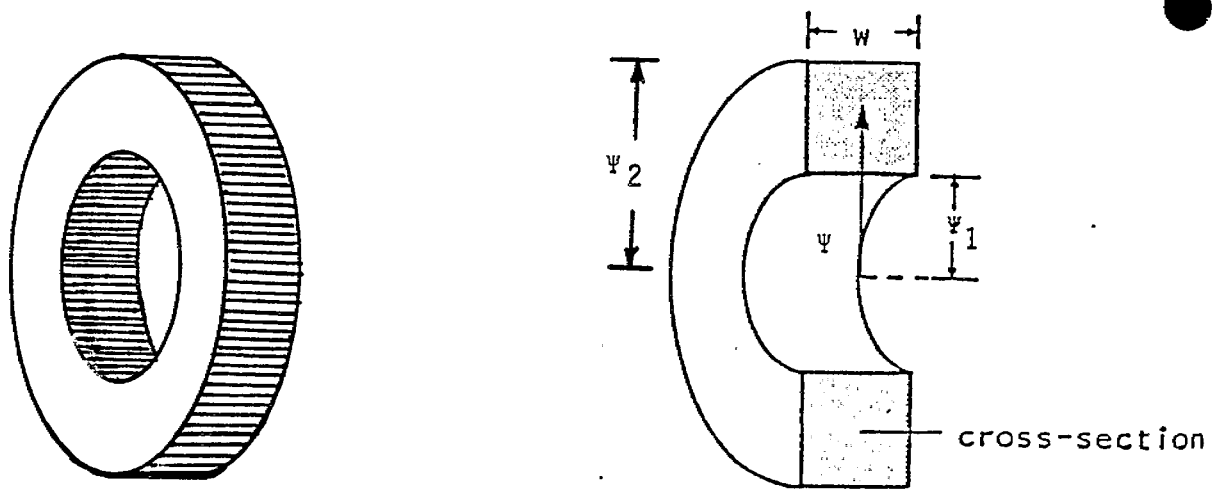


Figure 4.1 The ring shaped form.

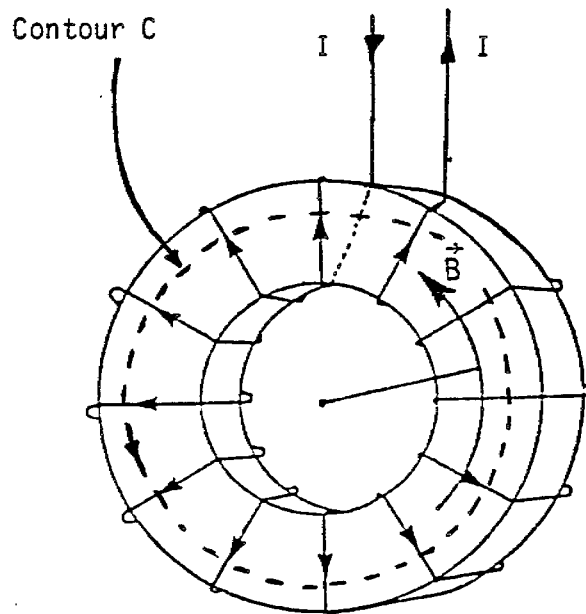


Figure 4.2 N_1 -turn winding and the magnetic field direction.

Next, we may consider a similar toroidal form but with a different winding arrangement as shown in figure 4.3. Once again, invoking Ampere's Law, we have

$$\oint_C \vec{B} \cdot d\vec{\ell} = \mu I(\text{enclosed}) \quad (4.5)$$

The current enclosed is now the number of turns N_2 times the current ($I/2$), leading to

$$B(\psi) = \mu N_2 \frac{I}{2} \frac{1}{2\pi\psi} \quad (4.6)$$

Note that symmetry enforces that equal currents $I/2$ flow between terminals A and B by the two parallel winding paths. Consider a rectangular cross section, in which the total flux is given as before by

$$\begin{aligned} \Phi &= \int_0^w dz \int_{\psi_1}^{\psi_2} \mu N_2 \frac{I}{2} \frac{1}{2\pi\psi} d\psi \\ &= w \frac{\mu}{2\pi} \frac{I}{2} N_2 \ln \left(\frac{\psi_2}{\psi_1} \right) \end{aligned} \quad (4.7)$$

The inductance L_2 of the toroid of figure 4.3 with two windings is easily written down as

$$L_2 = \frac{N_2}{2} \frac{\Phi}{I} = \frac{\mu}{8\pi} w N_2^2 \ln \left(\frac{\psi_2}{\psi_1} \right) \quad (4.8)$$

In computing the total flux, the cross sectional flux ϕ is multiplied by $(N_2/2)$ and not (N_2) since the number of turns in either of the two parallel paths between the terminals A and B is $(N_2/2)$.

The inductance L_2 can also be derived in an alternate way by equating energies as follows

$$\frac{1}{2} L_2 I^2 = U_m = \int \frac{1}{2} \mu H^2 dV \quad (4.9)$$

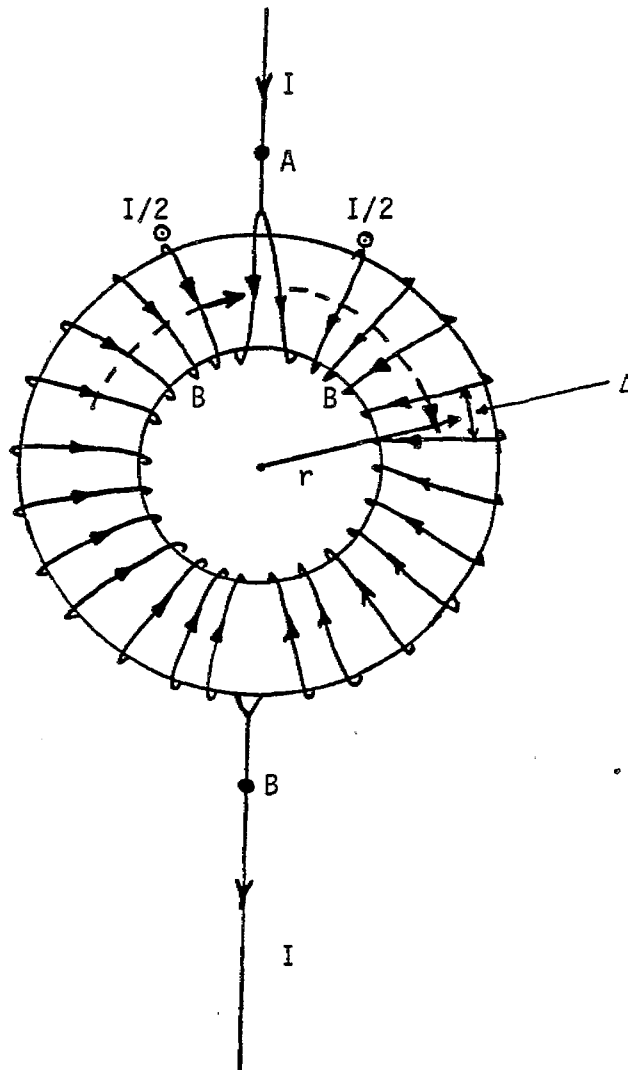


Figure 4.3 Toroidal form with $N_2/2$ turns of opposing winding senses in each half.

leading to

$$\begin{aligned}
 L_2 &= \frac{2}{I^2} \frac{1}{2} \int_0^w dz \int_{\Psi_1}^{\Psi_2} 2\pi\Psi \left(\frac{I}{2} \frac{N_2}{2\pi\Psi} \right)^2 d\Psi \\
 &= \frac{\mu}{8\pi} w N_2^2 \ln\left(\frac{\Psi_2}{\Psi_1}\right)
 \end{aligned} \tag{4.10}$$

which is the same result as (4.8).

Having looked at two possible winding arrangements, i.e., single winding of figure 4.2 and double winding of figure 4.3, several observations are in order.

- (i) For the same current I and same number of turns $N_1 = N_2$, the single-wound coil has 4 times more inductance than the double-wound coil.
- (ii) The stray capacitances associated with the double-wound coil is less than the single wound coil. Think of the turn-to-adjacent-turn capacitance, place $N_2/2$ of these in series, and place the two "halves" of the coil capacitance in parallel. This is an over simplified view and the advantage gained is actually not this great.
- (iii) The double-wound coil can be operated at a much higher voltage level since its terminals are at diametrically opposite points in the coil as opposed to being adjacent to each other in the single-wound case. In effect, the voltage is graded along the two "halves" of the coil with $N_2/2$ gaps instead of just one gap.

Items (ii) and (iii) above are the advantages of the double-wound coil, especially in simulator applications at the cost of reduced inductance for a given number of turns. This cost is not prohibitive since

$$L_1 = L_2 \text{ if } N_2 = 2N_1 \tag{4.11}$$

In other words, a double-wound coil with twice the number of turns has the same inductance as a single-wound coil, in addition to its enhanced suitability for high-voltage, low-capacitance applications.

Let us then focus our attention on a toroidal form with a rectangular cross section with a double winding similar to what appears in figure 4.3. The cross section of such a toroid is shown in figure 4.4. The inner and outer cylindrical 'radii' are Ψ_1 and Ψ_2 . The width of the form is w and it is inscribed in a spherical radius a as shown. A specification of w , Ψ_1 , Ψ_2 uniquely specifies the geometry and dependent parameters θ_0 and a , are also defined as indicated for the convenience of presenting the numerical results.

From the derivations in the earlier part of this section, the inductance L_2 of such a coil as shown in figure 4.4 under the assumption of a double winding in the sense of figure 4.3, is given by

$$L_2 \cong \frac{\mu}{8\pi} w N_2^2 \ln \left(\frac{\Psi_2}{\Psi_1} \right) \quad (4.12)$$

where N_2 is now the total number of turns in the entire coil with $N_2/2$ in each half wound in opposite senses.

In the next section, we start with (4.12) above and determine optimal shapes and also discuss related performance characteristics e.g., forces or pressure exerted.

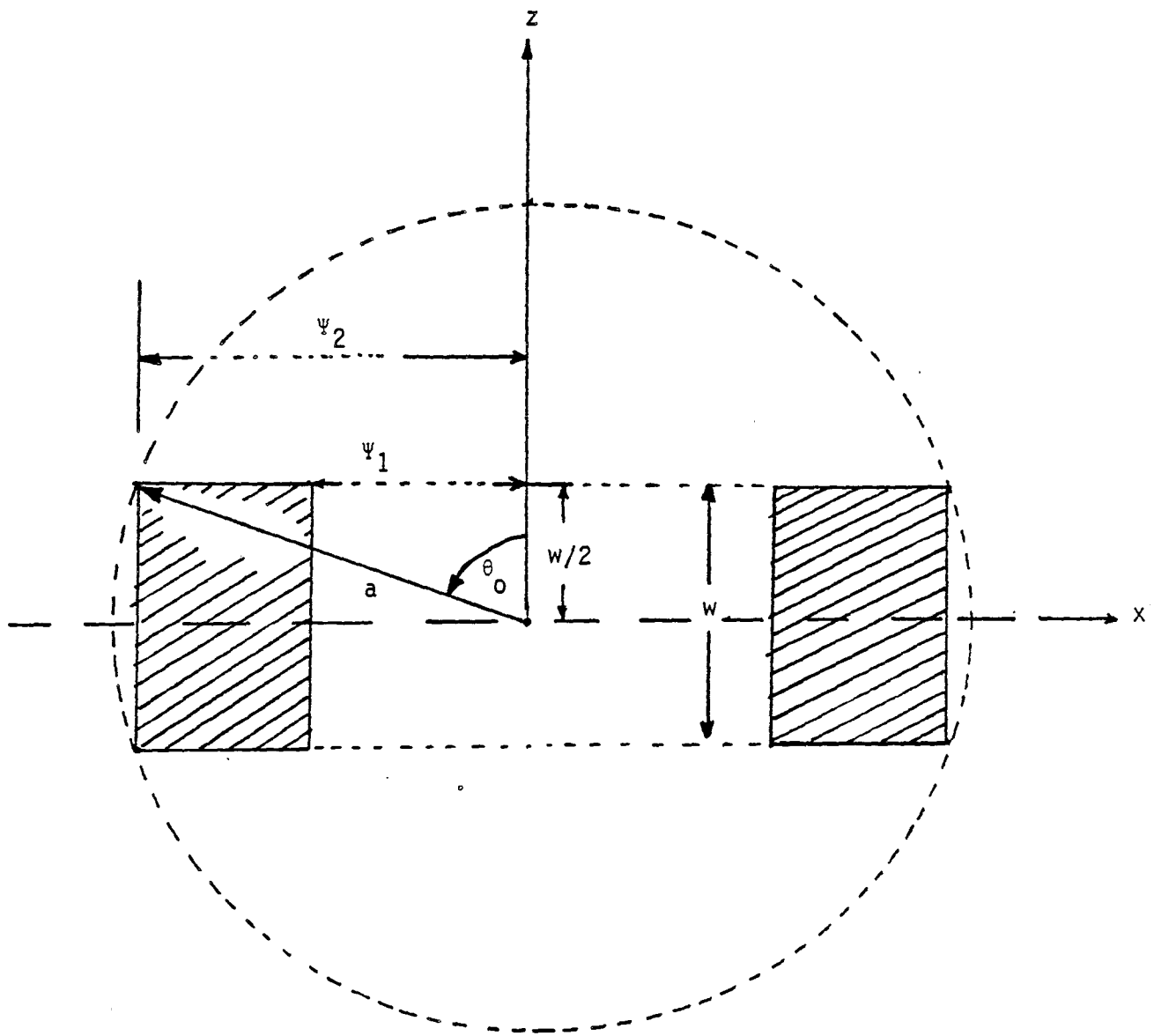


Figure 4.4 Rectangular cross section of a toroidal form and its geometrical parameters.

V. OPTIMUM SHAPE FOR CONTAINMENT IN FINITE SPHERICAL VOLUME AND OTHER PERFORMANCE CHARACTERISTICS

We start with the previously derived result for the inductance L of a coil with two windings, wound on a toroidal form of rectangular cross section. Ignoring the suffix '2', it is given by

$$L \cong \frac{\mu}{8\pi} w N^2 \ln\left(\frac{\psi_2}{\psi_1}\right) \quad (5.1)$$

The object now is to optimize this inductance with respect to geometrical parameters. Two independent geometrical parameters ζ and θ_0 are defined according as

$$\zeta = \psi_2/\psi_1 \quad (5.2)$$

and

$$\begin{aligned} \sin(\theta_0) &= \psi_2/a \\ \cos(\theta_0) &= w/(2a) \\ \tan(\theta_0) &= 2\psi_2/w \end{aligned} \quad (5.3)$$

Also, if Δ_1 is the minimum spacing between the turn centers at the inner boundary of the toroid, we have

$$N_{\max} \cong 2\pi\psi_1/\Delta_1 \quad (5.4)$$

Using N_{\max} in order to obtain the maximum possible L and also for improved field containment, we have

$$\begin{aligned}
L &\cong \frac{\mu\pi}{2} w \left(\frac{\psi_1}{\Delta_1}\right)^2 \ln\left(\frac{\psi_2}{\psi_1}\right) \\
&= \frac{\mu\pi w}{2\Delta_1^2} \psi_2^2 \frac{\ln(\zeta)}{\zeta^2} \\
&= \frac{\mu\pi w a^2}{2\Delta_1^2} \sin^2(\theta_0) \frac{\ln(\zeta)}{\zeta^2} \\
&= \frac{\mu\pi a^3}{\Delta_1^2} \cos(\theta_0) \sin^2(\theta_0) \frac{\ln(\zeta)}{\zeta^2}
\end{aligned} \tag{5.5}$$

If we make use of a change of variable

$$\cos(\theta_0) = v \tag{5.6}$$

(5.5) can be written as

$$L \cong \frac{\mu\pi a^3}{\Delta_1^2} v (1 - v^2) \frac{\ln(\zeta)}{\zeta^2} \tag{5.7}$$

It can be easily shown that L attains its maximum value L_{\max} when $v = 1/\sqrt{3}$ and $\zeta = \sqrt{e}$. With reference to figure 4.4, this corresponds to

$$\begin{aligned}
\cos(\theta_0) &= 0.5773 \text{ or } \theta_0 = 54.74^\circ \\
(\psi_2/\psi_1) &= 1.648
\end{aligned} \tag{5.8}$$

and

$$L_{\max} \cong \frac{\mu\pi a^3}{3\sqrt{3}e\Delta_1^2} = 0.222 \frac{\mu a^3}{\Delta_1^2} \tag{5.9}$$

Alternatively, for a specified L and Δ_1 , the minimum radius a_{\min} corresponding to the smallest spherical volume required to attain the specified L for a given Δ_1 is

$$a_{\min} = \left(4.5 \frac{L}{\mu} \Delta_1^2 \right)^{1/3} \quad (5.10)$$

(5.9) and (5.10) are useful when one is designing a specific inductor that is optimal.

We may also present the results of the inductance values in a set of normalized plots. Rewriting (5.5) in a normalized form, we have

$$L^{(n)} = \left(\frac{L \Delta_1^2}{\mu a^3} \right) = \pi \cos(\theta_0) \sin^2(\theta_0) \frac{\ln(\zeta)}{\zeta^2} \quad (5.11)$$

Observe that L_{norm} is a dimensionless parameter which could now be plotted as functions of θ_0 and ζ separately. These results are shown in Table 1 and plotted in figures 5.1 and 5.2. The maximum value of $L^{(n)}$ i.e., $L_{\text{max}}^{(n)}$ is observed to be 0.222 for $\theta_0 = 54.74^\circ$ and $\zeta = 1.648$ which is consistent with (5.9). The inductance equations and the results plotted are useful in actual design and fabrication of such field-containing inductors in high-voltage, low-capacitance applications.

Other related performance characteristics of these inductors are: (1) energy handling capacity and (2) force or pressure exerted in the toroidal form due to the current flow in the windings.

The energy capacity is simply governed by $(0.5 L I^2)$ and it is essentially the same as the single winding inductor carrying the same current, under the assumption of twice the number of turns in the double winding inductor.

With regards to the pressure (= Force per unit area) due to magnetic field, one may visualize such forces as originating from a tension T along the magnetic field lines and a pressure P at right angles to the magnetic field lines [5]. Both T and P are given numerically by

$$\begin{aligned} |T| &= |P| = \frac{B^2}{2\mu} = \frac{\mu H^2}{2} \\ &= \frac{\mu}{2} \left(\frac{NI}{4\pi r} \right)^2 \end{aligned} \quad (5.12)$$

TABLE 1
Normalized Inductance $L^{(n)}$ for
Varying Geometrical Parameters

θ_0 (degrees) \ $\xi = \psi_2 / \psi_1$	1.1	1.3	1.5	1.649	2	2.5	3	3.5	4	4.5	5
10	0.007	0.014	0.016	0.017	0.016	0.013	0.011	0.009	0.008	0.007	0.006
20	0.027	0.054	0.062	0.064	0.060	0.051	0.042	0.035	0.030	0.026	0.022
30	0.054	0.106	0.123	0.125	0.118	0.100	0.083	0.070	0.059	0.050	0.044
40	0.078	0.154	0.179	0.183	0.172	0.146	0.121	0.101	0.086	0.073	0.064
50	0.094	0.184	0.213	0.218	0.205	0.174	0.144	0.121	0.103	0.087	0.076
54.74	0.096	0.188	0.218	0.222	0.209	0.178	0.148	0.123	0.105	0.089	0.077
60	0.093	0.183	0.212	0.217	0.204	0.173	0.144	0.120	0.102	0.087	0.075
70	0.075	0.147	0.171	0.175	0.164	0.140	0.116	0.097	0.083	0.070	0.061
80	0.042	0.082	0.096	0.098	0.092	0.078	0.065	0.054	0.046	0.039	0.034

NOTE:

$$L^{(n)} = \left(\frac{L \Delta_1^2}{\mu a^3} \right)$$

L = inductance of the coil

Δ_1 = inner spacing between
turn centers

μ = permeability of the medium

a = spherical radius of the
coil

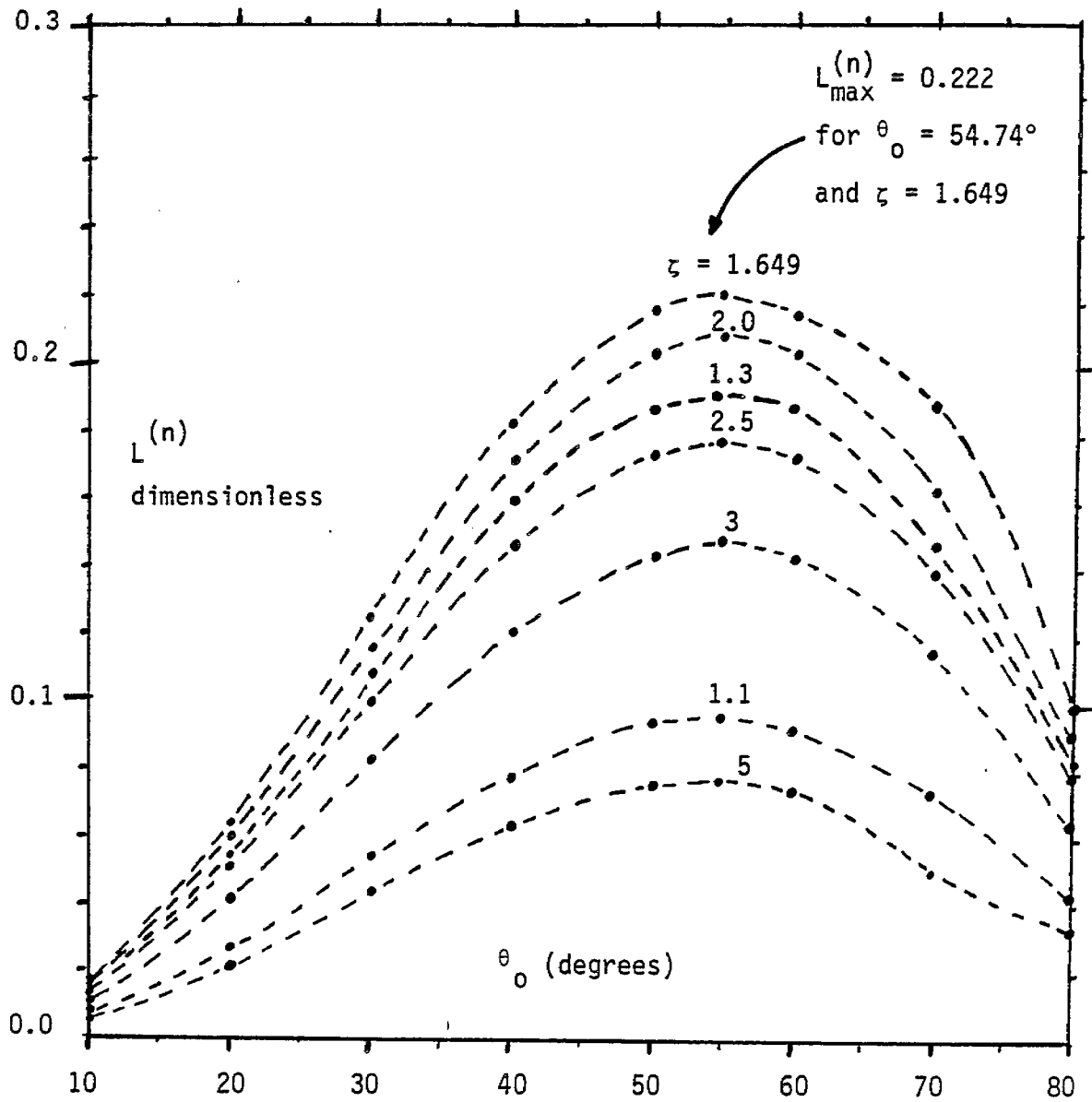


Figure 5.1 Normalized inductance as a function of θ_0 for various ζ ($= \psi_2/\psi_1$).

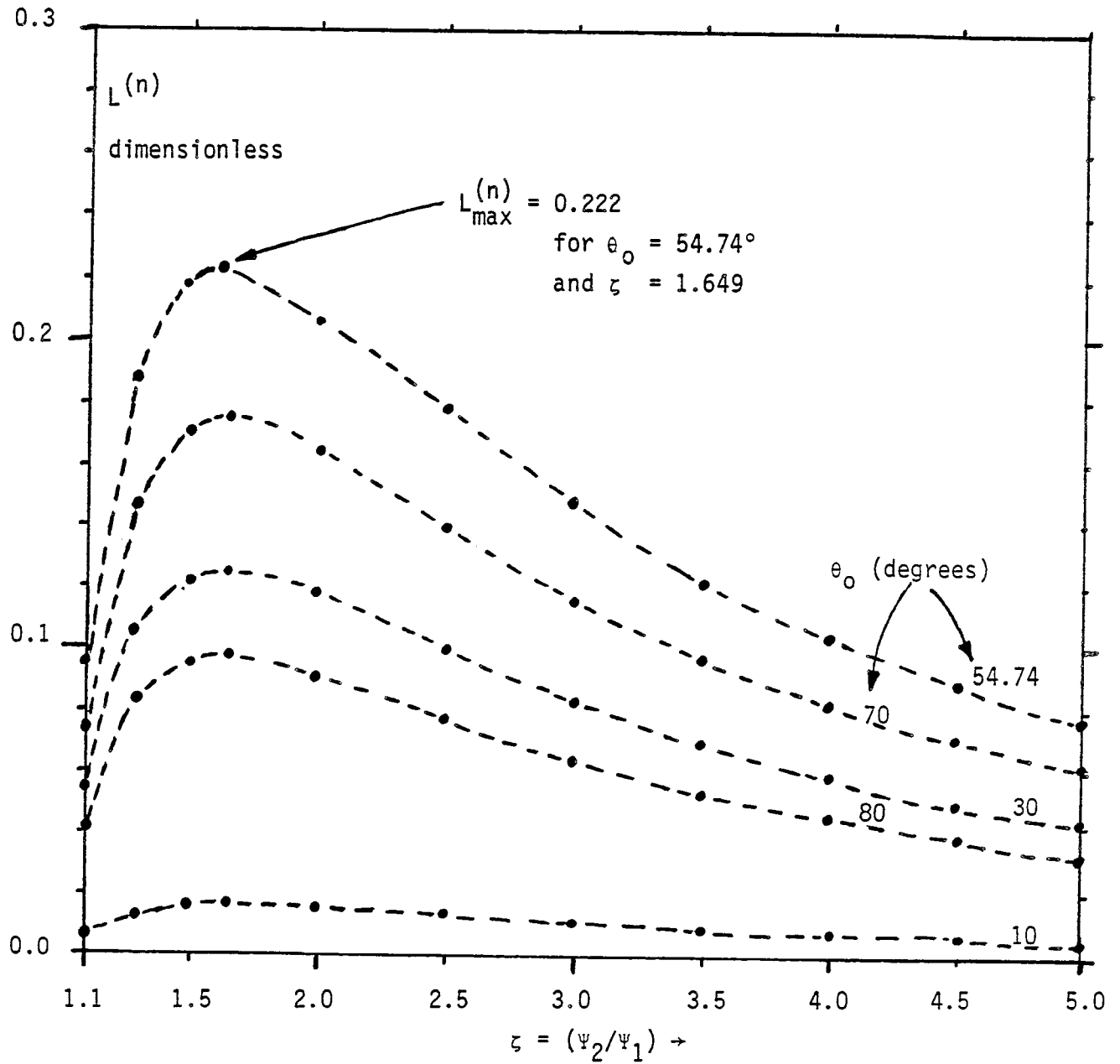


Figure 5.2 Normalized inductance as a function of ζ for various θ_0 .

In the present case, since B is oriented in the azimuthal or ϕ direction, the force is directed radially or axially, depending on which face of the rectangular cross section one is looking at. In any case, this force, quantified in (5.12) is present and tends to push the enclosing surface S in the direction of outward normal \vec{I}_S . If such forces become a concern, nonconducting mechanical restraints such as tubes, bands and weights may become necessary. It is also noted that the pressure is maximum at or near the inner boundary as given by

$$|P|_{\max} = \frac{\mu}{2} \left(\frac{NI}{4\pi\psi_1} \right)^2 = \frac{\mu}{8} \frac{I^2}{\Delta_1^2} \quad (5.13)$$

and the energy U_m is given by

$$U_m = \frac{1}{2} L I^2 \quad (5.14)$$

One could perhaps define a parameter δ which is the ratio of the maximum pressure to energy, as

$$\delta = \frac{|P|_{\max}}{U_m} = \frac{\mu}{4} \frac{1}{L\Delta_1^2} \quad (5.15)$$

It is desirable to minimize this ratio, which is accomplished by requiring a geometry that leads to the maximum inductance value, which has been previously discussed.

VI. SUMMARY

Typical solenoidal coils have large magnetic dipole moments leading to excessive interfering magnetic fields, in other regions of interest. In an effort to contain the magnetic field, toroidal forms with a single winding have been employed in the past. However such single winding coils are limited in their voltage handling capability since the applied voltage is graded essentially across the distance between adjacent turn centers.

Recent advancements in simulation technology have created a need for high-voltage, low-capacitance inductors, which is the problem addressed in this report. Design formulas are developed, normalized inductance values are plotted and performance characteristics such as energy considerations, pressure exerted due to current flow are discussed. It is also observed that such inductors have the added advantage of no mutual coupling between various inductors in a given circuit. For example, field-containing inductors can be added in series, parallel combinations and they will have very little mutual inductance, since none of them has an exterior magnetic field to couple into other inductors.

REFERENCES

1. C.E. Baum, "Some Characteristics of Electric and Magnetic Dipole Antennas for Radiating Transient Pulses," Sensor and Simulation Note 125, January 1971.
2. C.E. Baum, "Topological Considerations for Low-Frequency Shielding and Grounding," ELECTROMAGNETICS, Volume 3, Number 2, pp 145 - 157, April - June 1983, and as Interaction Note 417, June 1982.
3. S. Ramo, J.R. Whinnery and T. Van Duzer, Fields and Waves in Communication Electronics, John Wiley and Sons, Section 2.13, 1965.
4. F.W. Grover, Inductance Calculations, Working Formulas and Tables, Dover Publications, 1962.
5. W.R. Smythe, Static and Dynamic Electricity, McGraw-Hill Book Company, Inc., New York 1950.